

Low-mass Higgs decays to four leptons at one loop and beyond

Bernd A. Kniehl, Oleg L. Veretin

II. Institut für Theoretische Physik, Universität Hamburg,
Luruper Chaussee 149, 22761 Hamburg, Germany

Abstract

The ongoing searches for Higgs-boson signals in data taken at the CERN LHC and the Fermilab Tevatron crucially rely on the decay channels $H \rightarrow Z\ell\ell$ and $H \rightarrow W\ell\nu_\ell$. We present a precision study of the partial widths of these decay channels including the full one-loop electroweak corrections and the dominant contributions at two and three loops, of $\mathcal{O}(G_F^2 m_t^4)$, $\mathcal{O}(G_F m_t^2 \alpha_s)$, and $\mathcal{O}(G_F m_t^2 \alpha_s^2)$. Since the invariant mass of the off-shell intermediate boson is relatively low in the mass window $115 \text{ GeV} < m_H < 129 \text{ GeV}$ of current interest, lepton mass effects are relevant, especially for the τ lepton.

PACS numbers: 12.15.Lk, 12.38.Bx, 13.40.Ks, 14.80.Bn

1 Introduction

The ATLAS and CMS Collaborations at the pp collider LHC are presently closing in on the Higgs boson of the standard model (SM). The combined ATLAS results, based on the full data set of up to 4.9 fb^{-1} recorded during the 2011 operation at the center-of-mass energy $\sqrt{s} = 7 \text{ TeV}$, excluded the Higgs-boson mass (m_H) windows from 110.0 GeV to 117.5 GeV, from 118.5 GeV to 122.5 GeV, and from 129 GeV to 539 GeV at the 95% confidence level (CL) [1]. A small excess of signal events over the estimated background was observed around $m_H = 126 \text{ GeV}$ with a local significance of 2.5 standard deviations (σ). The CMS Collaboration excluded the m_H window from 127.5 GeV to 600 GeV at 95% CL exploiting approximately 5 fb^{-1} of data at $\sqrt{s} = 7 \text{ TeV}$ [2]. They observed some excess in the m_H window from 115 GeV to 128 GeV, with a maximum local significance of 2.8σ at $m_H = 125 \text{ GeV}$.

The CDF and D0 Collaborations at the $p\bar{p}$ collider Tevatron jointly excluded the m_H windows from 100 GeV to 106 GeV and from 141 GeV to 184 GeV at 95% CL by analyzing a luminosity of up to 10 fb^{-1} collected at $\sqrt{s} = 1.96 \text{ TeV}$ [3]. They observed an excess of signal over background in the m_H window from 115 GeV to 135 GeV, with a local significance of 2.2σ at $m_H = 120 \text{ GeV}$. The ALEPH, DELPHI, L3, and OPAL Collaborations at the CERN e^+e^- collider LEP established a m_H lower bound of 114.4 GeV at 95% CL using a total of 2.461 fb^{-1} data collected at $189 \text{ GeV} < \sqrt{s} < 209 \text{ GeV}$ [4].

The searches at the LHC for the SM Higgs boson in the low- m_H region mainly rely on its decay channels $H \rightarrow \gamma\gamma$ [5,6], $H \rightarrow ZZ^* \rightarrow \ell^+\ell^-\ell'^+\ell'^-$ [7,8], $H \rightarrow W^+W^{*-}, W^-W^{+*} \rightarrow \ell^+\nu_\ell\ell'^-\bar{\nu}_{\ell'}$ [9,10], where off-mass-shell particles are marked by asterisks and $\ell, \ell' = e, \mu$. Decay channels of lesser significance include $H \rightarrow \tau^+\tau^-$ [11] and, in $W^\pm H$ and ZH associated production with subsequent $W^\pm \rightarrow \ell^\pm(\bar{\nu}_\ell)$ and $Z \rightarrow \ell^+\ell^-$ decays, $H \rightarrow b\bar{b}$ [12]. In the following, we briefly review the state of the art regarding the theoretical predictions for the respective partial decay width. Comprehensive reviews of our theoretical knowledge of the SM Higgs boson may be found in Refs. [13,14] and references cited therein.

As for the partial width $\Gamma(H \rightarrow \gamma\gamma)$, the lowest-order result was first obtained in Ref. [15]. The two-loop $\mathcal{O}(\alpha_s)$ [16] and three-loop $\mathcal{O}(\alpha_s^2)$ [17] QCD corrections are available. As for the two-loop $\mathcal{O}(\alpha)$ correction, the contributions induced by light [18] and heavy fermions [19,20] as well as the residual ones [21] are known.

As for the partial decay width $\Gamma(H \rightarrow b\bar{b})$, the one-loop $\mathcal{O}(\alpha_s)$ [22] and $\mathcal{O}(\alpha)$ [23,24] corrections have been known for a long time. As for the two-loop $\mathcal{O}(\alpha_s^2)$ correction, the leading [25] and next-to-leading [26] terms of the expansion in m_b^2/m_H^2 of the diagrams without top quarks are known. The diagrams containing a top quark can be divided into two classes: diagrams containing gluon self-energy insertions, which are exactly known [27], and double-triangle diagrams, for which the four leading terms of the expansion in m_H^2/m_t^2 are known [28]. As for the two-loop correction of order $\mathcal{O}(x_t\alpha_s)$, where $x_t = G_F m_t^2/(8\pi^2\sqrt{2})$ parametrizes leading power corrections of top-quark origin, the universal part, which appears for any Higgs-boson decay to a fermion pair, was extracted from the full $\mathcal{O}(\alpha\alpha_s)$ result [29] and the non-universal one, which arises because bottom is the isopartner of top, using a low-energy theorem [30]. As for the two-loop $\mathcal{O}(x_t^2)$ correction,

the universal [19,31] and non-universal [31] parts are both available. The three-loop $\mathcal{O}(\alpha_s^3)$ correction without top-quark contribution was calculated in the massless limit [32]. The correction induced by the top quark was subsequently found using an appropriate effective field theory [33]. As for the three-loop $\mathcal{O}(x_t\alpha_s^2)$ correction, the universal [34] and non-universal [35] parts are both known. The four-loop $\mathcal{O}(\alpha_s^4)$ correction without top-quark contribution was calculated in the massless limit [36]. The residual theoretical uncertainty in the prediction of $\Gamma(H \rightarrow b\bar{b})$ was assessed in Ref. [37].

As for the partial decay width $\Gamma(H \rightarrow \tau^+\tau^-)$, we know the full one-loop $\mathcal{O}(\alpha)$ [23,24] and two-loop $\mathcal{O}(\alpha\alpha_s)$ [29] corrections as well as the dominant two-loop $\mathcal{O}(x_t^2)$ [19] and three-loop $\mathcal{O}(x_t\alpha_s^2)$ [34] terms.

The decays of the Higgs boson to two pairs of light fermions proceed almost exclusively via a $W^{(*)}W^{(*)}$ or $Z^{(*)}Z^{(*)}$ pairs, the contributions involving the Yukawa couplings of the produced fermions being greatly suppressed, as will be explicitly demonstrated for $H \rightarrow Z\tau^+\tau^-$ and $H \rightarrow W^+\tau^-\bar{\nu}_\tau$ in Sec. 3. If the value of m_H is large enough to allow for one or both intermediate bosons to be on mass shell, then such kinematic configurations will be extremely favored due to the resonating propagators [38]. In this case it is natural to employ the narrow-width approximation, which implies that the resonating intermediate bosons are treated as real particles and their subsequent decays are accounted for by multiplication with the appropriate branching fractions. Such a procedure is also routinely employed when the cross section of a complete scattering process involving the unstable Higgs boson is factorized into the cross section of the Higgs-boson production mechanism and the branching fraction of the Higgs-boson decay channel. In the case of Higgs-boson decays to two light-fermion pairs, this has the advantage that the branching fractions $B(Z \rightarrow f\bar{f})$ and $B(W^\pm \rightarrow f\bar{f}')$ may be taken to be the experimentally measured values, which naturally contain all radiative corrections. As for the partial decay widths $\Gamma(H \rightarrow W^+W^-)$ and $\Gamma(H \rightarrow ZZ)$, which presuppose that $m_H > 2m_V$ with $V = W, Z$, the full one-loop $\mathcal{O}(\alpha)$ corrections [23,39,40,41], also including the subsequent decays into massless-fermion pairs [42], the dominant two-loop terms of $\mathcal{O}(x_t^2)$ [19] and $\mathcal{O}(x_t\alpha_s)$ [43,44], and the three-loop term of $\mathcal{O}(x_t\alpha_s^2)$ [34] are available.

The purpose of this paper is to present a precision study of the partial decay widths $\Gamma(H \rightarrow W^\pm f\bar{f}')$ and $\Gamma(H \rightarrow Zf\bar{f})$, appropriate for the mass window $m_V < m_H < 2m_V$ of topical interest, retaining the masses of the produced fermions and including the full one-loop corrections and the dominant higher-order terms. In the case of $H \rightarrow Zf\bar{f}$ with massless final-state fermions, the one-loop weak correction may be obtained [13] by crossing symmetry from the corresponding analysis of $e^+e^- \rightarrow ZH$ [45]. Here, we redo this calculation for massive final-state fermions and incorporate the $\mathcal{O}(x_t^2)$, $\mathcal{O}(x_t\alpha_s)$, and $\mathcal{O}(x_t\alpha_s^2)$ terms. We also perform the analogous analysis for $H \rightarrow W^\pm f\bar{f}'$. In fact, the numerical analyses for $H \rightarrow Z\tau^+\tau^-$ and $H \rightarrow W^+\tau^-\bar{\nu}_\tau$ in Sec. 3 will reveal that the finite τ -lepton mass effects may exceed the radiative corrections in size in the low- m_H window that is not excluded experimentally. Both channels are bound to be exploited for the search of a low- m_H Higgs boson and/or the study of its properties in the long run. The $H \rightarrow \ell^+\ell^-\tau^+\tau^-$ channel is already being used by the CMS Collaboration in the high- m_H range [46].

This paper is organized as follows. In Sec. 2, we expose the structure of our analytical results and list an appropriate selection of our formulas. In Sec. 3, we present our numerical analysis for the $H \rightarrow W^+ \ell^- \bar{\nu}_\ell$ and $H \rightarrow Z \ell^+ \ell^-$ decay channels, which are relevant for the ongoing searches for Higgs-boson signals in data taken at the LHC and the Tevatron. In Sec. 4, we summarize our conclusions.

2 Analytic results

We now present our analytic results. We work in the on-mass-shell renormalization scheme implemented with Fermi's constant G_F , instead of Sommerfeld's fine-structure constant α , and use the short-hand notations $h = M_H^2$, $w = M_W^2$, $z = M_Z^2$, and $c_w^2 = 1 - s_w^2 = w/z$.

2.1 $H \rightarrow Z f \bar{f}$ decay

We first consider the decay process $H \rightarrow Z f \bar{f}$ for a generic fermion f of mass m , electric charge Q , and color multiplicity N , which is $N = 1$ for leptons and $N = 3$ for quarks. The $Z f \bar{f}$ vector and axial-vector couplings are proportional to $V = 2I - 4s_w^2 Q$ and $A = 2I$, where $I = \pm 1/2$ is the third component of weak isospin of the left-handed component of f . Formally, the partial decay width of $H \rightarrow Z f \bar{f}$ and the one of $Z \rightarrow H f \bar{f}$, the radiative corrections to which were studied in Ref. [47], are related as [13]

$$\Gamma_{H \rightarrow Z f \bar{f}} = -3 \left(\frac{z}{h} \right)^{3/2} \Gamma_{Z \rightarrow H f \bar{f}}, \quad (1)$$

where the minus sign ensures that the phase space remains positive upon the interchange $z \leftrightarrow h$, and the factors 3, $\sqrt{z/h}$, and z/h adjust the spin average, flux, and phase space, respectively. In contrast to Ref. [47], we include here also the finite- m corrections.

The distribution of the partial decay width $\Gamma_{H \rightarrow Z f \bar{f}}$ in the $f \bar{f}$ invariant mass square $s = q^2$ may be written as

$$\frac{d\Gamma_{H \rightarrow Z f \bar{f}}}{ds} = \frac{d\Gamma_{H \rightarrow Z f \bar{f}}^0}{ds} \left[\delta_0 + \frac{3}{4} \left(\frac{\alpha}{\pi} Q^2 + \frac{\alpha_s}{\pi} C_F \right) \delta_1 + \delta_w - \delta_{x_t} + \delta_{\text{res}} \right] \delta_t, \quad (2)$$

where

$$\frac{d\Gamma_{H \rightarrow Z f \bar{f}}^0}{ds} = \frac{G_F^2 z^3}{128 \pi^3 h^{3/2}} N (V^2 + A^2) \frac{C_1}{(s - z)^2}, \quad (3)$$

with $C_1 = \sqrt{\lambda} [4s + \lambda/(3z)]$ [45] and $\lambda = s^2 + z^2 + h^2 - 2(sz + zh + hs)$, is the tree-level result for $m = 0$ [48,49], the factor δ_0 restores the full m dependence of the latter, δ_1 is the coefficient shared by the $\mathcal{O}(\alpha)$ QED and $\mathcal{O}(\alpha_s)$ QCD corrections, δ_w contains the purely weak correction at one loop, δ_{x_t} is the leading $\mathcal{O}(x_t)$ term of the latter, the factor δ_t supplies the leading top-quark-induced corrections at one loop and beyond, and δ_{res} comprises the residual higher-order corrections, which are beyond the scope our present analysis.

It is useful to distinguish between the class of contributions devoid of the $Hf\bar{f}$ Yukawa coupling and the complementary class. The former survives in the massless limit $m \rightarrow 0$, and the parts of δ_0 and δ_1 that belong to it are related via the optical theorem to the absorptive part of the Z -boson vacuum polarization tensor induced by the fermion f ,

$$\Pi^{\mu\nu}(q) = g^{\mu\nu}\Pi_T(s) + q^\mu q^\nu \Pi_L(s), \quad (4)$$

where

$$\Pi_i(s) = \frac{G_F z}{2^{3/2}} [V^2 \Pi_i^V(s) + A^2 \Pi_i^A(s)]. \quad (5)$$

While, for $m = 0$, only the transversal part $\Pi_T(s)$ matters, the longitudinal part $\Pi_L(s)$, too, is relevant for $m > 0$. Due to vector current conservation, we have

$$\Pi_T^V(s) + s\Pi_L^V(s) = 0, \quad (6)$$

so that we have to consider only three different coefficient functions. Through the two-loop order, we have [50,51,52]

$$\begin{aligned} \text{Im } \Pi_T^V(s) &= \frac{s}{12\pi} N \left[v_0(r) + \frac{3}{4} \left(\frac{\alpha}{\pi} Q^2 + \frac{\alpha_s}{\pi} C_F \right) v_1(r) \right], \\ \text{Im } \Pi_T^A(s) &= \frac{s}{12\pi} N \left[a_0(r) + \frac{3}{4} \left(\frac{\alpha}{\pi} Q^2 + \frac{\alpha_s}{\pi} C_F \right) a_1(r) \right], \\ \text{Im } \Pi_L^A(s) &= \text{Im } \Pi_L^V(s) - \frac{1}{12\pi} N \left[l_0(r) + \frac{3}{4} \left(\frac{\alpha}{\pi} Q^2 + \frac{\alpha_s}{\pi} C_F \right) l_1(r) \right], \end{aligned} \quad (7)$$

where $C_F = (N^2 - 1)/(2N)$,

$$v_0(r) = \rho \left(1 + \frac{1}{2r} \right), \quad a_0(r) = \rho^3, \quad l_0(r) = 0, \quad (8)$$

$rv_1(r)$ and $ra_1(r)$ are given by Eqs. (5) and (6) in Ref. [51], respectively, $-l_1(r)/(4\pi)$ is given by the second term on the right-hand side of Eq. (13) in Ref. [52], $r = s/(4m^2)$, and $\rho = \sqrt{1 - 1/r}$. In Eq. (7), the normalizations are arranged so that $v_i(\infty) = a_i(\infty) = 1$ ($i = 0, 1$), while we have $l_1(r) = 1/r^2 + \mathcal{O}(1/r^3)$ for $r \gg 1$.

The correction terms in Eq. (2) may now be presented in a compact form. Specifically, we have

$$\delta_i = \frac{1}{V^2 + A^2} \left\{ V^2 v_i(r) + A^2 a_i(r) + \frac{(s - z)^2}{C_1} \left[-\frac{\lambda^{3/2}}{3z^3} A^2 (a_i(r) - v_i(r) - l_i(r)) + y_i \right] \right\}, \quad (9)$$

where y_0 and y_1 represent respectively the tree-level and one-loop corrections involving one or two powers of the $Hf\bar{f}$ Yukawa coupling. For $m = 0$, we have $\delta_i = 1$, so that $\delta_i - 1$ measures the relative finite- m correction at tree level ($i = 0$) or at one loop in QED and

QCD ($i = 1$). For y_0 , we find

$$y_0 = \frac{2m^2}{z^2(z-s)} \left\{ \rho\sqrt{\lambda} \left[- (V^2(z+2m^2) + A^2(z-4m^2)) \frac{s(z-s)(h-4m^2)}{hzs+m^2\lambda} - 4V^2z + A^2 \right. \right. \\ \times \left(6z+s - \frac{s}{z}(2h-s) \right) \left. \right] + V^2L \left[3z^2 - z(7h-6s) - 2h^2 - hs - s^2 + 4m^2(5h+2s) \right. \\ \left. - 16m^4 + 2h \frac{h^2 - 2m^2(5h-2s) + 8m^4}{h+z-s} \right] + A^2L \left[3z^2 + z(h+6s) + (h-s)(2h+s) \right. \\ \left. - 2m^2 \left(13z - h + 6s + \frac{(h-s)(2h-s)}{z} \right) + 32m^4 - 2h \frac{h^2 - 4m^2(h+s) + 16m^4}{h+z-s} \right] \left. \right\}, \quad (10)$$

where

$$L = \ln \frac{h+z-s-\rho\sqrt{\lambda}}{h+z-s+\rho\sqrt{\lambda}}. \quad (11)$$

As we shall see in Sec. 3, the contribution to δ_0 proportional to y_0 is exceedingly small. Our result for y_1 is too lengthy to be presented here.

Furthermore, we have

$$\delta_w = 2 \operatorname{Re} \Delta_{\text{weak}} + \delta_m, \quad (12)$$

where the $m = 0$ part Δ_{weak} is listed in analytic form in Ref. [45] and δ_m comprises the finite- m correction. We include δ_m in our numerical analysis, although it turns out to be small against Δ_{weak} , but we refrain from presenting here our analytic expression for it because it is too lengthy.

Finally, using the improved Born approximation (IBA) [53], we obtain

$$\delta_t = \frac{(1 + \delta_{ZZH})^2}{1 - \Delta\rho} \frac{(V - 4c_w^2 Q \Delta\rho)^2 + A^2}{V^2 + A^2} \\ = 1 + 2\delta_{ZZH} + (1 - 8X)\Delta\rho + \delta_{ZZH}^2 + 2(1 - 8X)\delta_{ZZH}\Delta\rho + (1 - 8X + 16Y)(\Delta\rho)^2 \\ + \mathcal{O}(x_t^3), \quad (13)$$

where $(1 + \delta_{ZZH})$ is the correction to the heavy-top-quark effective Lagrangian of the ZZH interaction, $\Delta\rho = 1 - 1/\rho$ measures the deviation of the electroweak ρ parameter from unity, $X = c_w^2 QV/(V^2 + A^2)$, and $Y = c_w^4 Q^2/(V^2 + A^2)$. Including the corrections of $\mathcal{O}(x_t)$ [23,40,41,54,55], $\mathcal{O}(x_t^2)$ [19,56], $\mathcal{O}(x_t\alpha_s)$ [44,57], and $\mathcal{O}(x_t\alpha_s^2)$ [34,58], we have

$$\delta_{ZZH} = x_t \left\{ -\frac{5}{2} - \left[\frac{177}{8} + 18\zeta(2) \right] x_t + [15 - 2\zeta(2)]a_s + 17.117 a_s^2 \right\}, \\ \Delta\rho = x_t \left\{ 3 + 3[19 - 12\zeta(2)]x_t - 2[1 + 2\zeta(2)]a_s - 43.782 a_s^2 \right\}, \quad (14)$$

where $\zeta(2) = \pi^2/6$ and $a_s = \alpha_s^{(6)}(m_t)/\pi$. Analytic expressions for the $\mathcal{O}(x_t\alpha_s^2)$ terms in Eq. (14) may be found in Refs. [34,58]. To avoid double counting, the $\mathcal{O}(x_t)$ term of Eq. (13) [45,47],

$$\delta_{x_t} = -2x_t(1 + 12X), \quad (15)$$

is subtracted in Eq. (2).

A more conservative form of Eq. (2) is obtained by discarding the quantities δ_{x_t} and δ_t , and in turn introducing within the square brackets the term δ_{ho} that contains the leading top-quark-induced corrections beyond one loop. In the leptonic case $f = l$, which is of special interest here, we have

$$\begin{aligned}\delta_{\text{ho}} &= \delta_t - 1 - \delta_{x_t} \\ &= \{13 - 72\zeta(2) + 24[-17 + 12\zeta(2)]X + 144Y\}x_t^2 \\ &\quad + 4\{7 - 2\zeta(2) + 4[1 + 2\zeta(2)]X\}x_t a_s + (-9.548 + 350.257X)x_t a_s^2.\end{aligned}\quad (16)$$

Finally, $\Gamma_{H \rightarrow Z f \bar{f}}$ is obtained by integrating Eq. (2) over the interval $4m^2 < s < (M_H - M_Z)^2$. The tree-level result for $m = 0$ reads [49]

$$\Gamma_{H \rightarrow Z f \bar{f}}^0 = \frac{G_F^2 z^4}{128\pi^3 h^{3/2}} N(V^2 + A^2) \left[-F\left(\frac{h}{z}\right) \right], \quad (17)$$

where $F(x)$ is given in Eq. (3) of Ref. [47].¹ For the reader's convenience, we reproduce this formula here:

$$\begin{aligned}F(x) &= \frac{1-x}{x} \left(-\frac{47}{2} + \frac{13}{2}x - x^2 \right) + \left(-2 + 3x - \frac{x^2}{2} \right) \ln x \\ &\quad + \left(10 - 4x + \frac{x^2}{2} \right) \sqrt{\frac{x}{4-x}} \left(\pi - 6 \arcsin \frac{\sqrt{x}}{2} \right).\end{aligned}\quad (18)$$

The origin of the minus sign on the right-hand side of Eq. (17) is explained in Eq. (1).

2.2 $H \rightarrow W^+ f \bar{f}'$ decay

We now consider the decay process $H \rightarrow W^+ f \bar{f}'$, where f is a generic fermion with weak isospin $I = -1/2$ and f' is an appropriate fermion with $I = 1/2$. By charge-conjugation invariance, the process $H \rightarrow W^- f' \bar{f}$ has the same partial decay width.

Some of the expressions for $H \rightarrow Z f \bar{f}$ in Sec. 2.1 carry over to $H \rightarrow W^+ f \bar{f}'$. Specifically, the counterparts of Eqs. (1), (3), (4), (5), and (17) are obtained by substituting $z \rightarrow w$ and $V, A \rightarrow \sqrt{2}$, and including the overall factor $|V_{f'f}|^2$, where $V_{f'f}$ is the Cabibbo-Kobayashi-Maskawa quark mixing matrix, if f and f' are quarks. However, structural differences occur because the intermediate boson is now electrically charged. In particular, the separation of QED and weak corrections is no longer meaningful at one loop because the photonic loop diagrams, including the appropriate counterterm diagrams, do no longer form a gauge-independent and ultraviolet-finite subset [13,39]. Furthermore, in the case when f and f' are quarks, the one-loop QCD correction is no longer proportional

¹The journal publication [47], this equation contains a misprint, which is absent in the preprint: $\sqrt{\frac{1}{4}x - x}$ should be replaced by $\sqrt{\frac{x}{4-x}}$.

to the QED correction. As a consequence, the distribution of the partial decay width $\Gamma_{H \rightarrow W^+ f \bar{f}'}$ in the $f \bar{f}'$ invariant mass square $s = q^2$ now takes the form

$$\frac{d\Gamma_{H \rightarrow W^+ f \bar{f}'}}{ds} = \frac{d\Gamma_{H \rightarrow W^+ f \bar{f}'}}{ds}^0 \left(\delta_0 + \frac{3}{4} \frac{\alpha_s}{\pi} C_F \delta_1 + \delta_{\text{ew}} - \delta_{x_t} + \delta_{\text{res}} \right) \delta_t. \quad (19)$$

In view of $m_\nu \ll m_\ell$ and $m_s \ll m_c$, we may safely neglect the mass of the lighter one of the two fermions f and f' and call the mass of the heavier one m . Due to the γ_5 reflection property $\Pi_i^V(s, m_1, m_2) = \Pi_i^A(s, m_1, -m_2)$ ($i = T, L$), we then have [50,51,52]

$$\Pi_i^V(s) = \Pi_i^A(s). \quad (20)$$

Through the two-loop order, we have [50,51,52]

$$\begin{aligned} \text{Im } \Pi_T^V(s) &= \frac{s}{12\pi} N \left[f_0(x) + \frac{3}{4} \frac{\alpha_s}{\pi} C_F f_1(x) \right], \\ \text{Im } \Pi_L^V(s) &= -\frac{1}{12\pi} N \left[g_0(x) + \frac{3}{4} \frac{\alpha_s}{\pi} C_F g_1(x) \right], \end{aligned} \quad (21)$$

where

$$f_0(x) = \left(1 + \frac{1}{2x}\right) \left(1 - \frac{1}{x}\right)^2, \quad g_0(x) = \left(1 + \frac{2}{x}\right) \left(1 - \frac{1}{x}\right)^2, \quad (22)$$

$xf_1(x)/4$ is given by Eq. (7) in Ref. [51], $-g_1(x)/4$ is given by Eq. (14) in Ref. [52], and $x = s/m^2$. In Eq. (7), the normalizations are arranged so that $f_i(\infty) = g_i(\infty) = 1$ ($i = 0, 1$).

Then, we have

$$\delta_i = f_i(x) + \frac{(s-w)^2}{C_1} \left\{ -\frac{\lambda^{3/2}}{3w^3} [f_i(x) - g_i(x)] + y_i \right\}, \quad (23)$$

where C_1 and λ are defined as below Eq. (3), but with z replaced by w . For y_0 , we find

$$\begin{aligned} y_0 &= \frac{m^2}{2w^3 s^2 (w-s)} \left\{ \sqrt{\lambda} \left[s^3 (3w+s) - 2h(s-m^2)(s^2 + 2m^2(w-s)) + 2m^2 w(w+s) \right. \right. \\ &\quad \times (s-2m^2) + \frac{m^2 s^2 (w-s)(2w+m^2)(w+s-2m^2)^2}{h(w-m^2)(s-m^2) + m^2(w-s)^2} \Big] + s^2 L \left[2w(3w(-h+w+2s) \right. \\ &\quad \left. \left. - s(h+s)) + m^2(w(9h-5w-2s) + s(3h-s)) - 4m^4(h+w+s) \right] \right\}, \end{aligned} \quad (24)$$

where

$$L = \ln \frac{(s+m^2)(w-s) + (s-m^2)(h-\sqrt{\lambda})}{(s+m^2)(w-s) + (s-m^2)(h+\sqrt{\lambda})}. \quad (25)$$

As will be shown in Sec. 3, the contribution proportional to y_0 is very small compared to δ_0 . For lack of space, we do not present y_1 and δ_{ew} in analytic form. Furthermore, we have

$$\delta_t = (1 + \delta_{WWH})^2. \quad (26)$$

Including the corrections of $\mathcal{O}(x_t)$ [23,39,41,54], $\mathcal{O}(x_t^2)$ [19], $\mathcal{O}(x_t\alpha_s)$ [43], and $\mathcal{O}(x_t\alpha_s^2)$ [34], we have

$$\delta_{WWH} = x_t \left\{ -\frac{5}{2} + \left[\frac{39}{8} - 18\zeta(2) \right] x_t + [9 - 2\zeta(2)]a_s + 27.041 a_s^2 \right\}. \quad (27)$$

An analytic expression for the $\mathcal{O}(x_t\alpha_s^2)$ term may be found in Ref. [34]. The $\mathcal{O}(x_t)$ term of Eq. (26) is

$$\delta_{x_t} = -5x_t. \quad (28)$$

Again, we may trade the quantities δ_{x_t} and δ_t in Eq. (19) against the term δ_{ho} , carrying the leading top-quark-induced corrections beyond one loop, to be inserted within the parentheses. In the leptonic case, we have

$$\begin{aligned} \delta_{\text{ho}} &= \delta_t - 1 - \delta_{x_t} \\ &= 4[4 - 9\zeta(2)]x_t^2 + 2[9 - 2\zeta(2)]x_t a_s + 54.082 x_t a_s^2. \end{aligned} \quad (29)$$

Finally, $\Gamma_{H \rightarrow W^+ f \bar{f}'}$ is obtained by integrating Eq. (19) over the interval $m^2 < s < (M_H - M_W)^2$.

3 Numerical results

We are now in a position to explore the phenomenological consequences of our results by performing a numerical analysis. We adopt all the input parameter values from Ref. [59]. Specifically, we use $m_W = 80.399$ GeV, $m_Z = 91.1876$ GeV, $m_b = 4.78$ GeV, $m_t = 172.9$ GeV, and $\alpha_s^{(6)}(m_t) = 0.1080$, which follows from $\alpha_s^{(5)}(m_Z) = 0.1184$ via four-loop evolution and three-loop matching [60]. In our renormalization scheme, $\sin^2 \theta_w = 1 - m_W^2/m_Z^2 = 0.222627$ and $\alpha = \sqrt{2}G_F \sin^2 \theta_w m_W^2/\pi = 1/132.349$ are derived parameters.

We first consider the $H \rightarrow Z\ell^+\ell^-$ decays. In Fig. 1, we present the tree-level finite- m (dotted lines) and radiative (solid lines) corrections to (a) $d\Gamma(H \rightarrow Z\tau^+\tau^-)/ds$ for $m_H = 125$ GeV as functions of \sqrt{s} , and to (b) $\Gamma(H \rightarrow Z\tau^+\tau^-)$ and (c) $\Gamma(H \rightarrow Z\mu^+\mu^-)$ as functions of m_H . The radiative corrections are decomposed into the $\mathcal{O}(\alpha)$ QED (coarsely dotted lines), $\mathcal{O}(\alpha)$ weak (dashed lines), and dominant higher-order (dot-dashed lines) corrections, of $\mathcal{O}(x_t^2)$, $\mathcal{O}(x_t\alpha_s)$, and $\mathcal{O}(x_t\alpha_s^2)$. For comparison, the $\mathcal{O}(\alpha)$ corrections predicted by the IBA (dot-dot-dashed lines) are also shown. Looking at Fig. 1(a), we observe that the QED correction $3\alpha\delta_1/(4\pi)$ exhibits an enhancement towards low values of \sqrt{s} , which is of Coulomb origin, while it gets close to its asymptotic value $3\alpha/(4\pi)$ as \sqrt{s} approaches its kinematic upper bound. The purely weak correction δ_w monotonically increases with \sqrt{s} , ranging from slightly negative values at the $\tau^+\tau^-$ pair production threshold to about 2.1% at the upper endpoint. The one-loop electroweak correction is inadequately described by the IBA term δ_{x_t} . The dominant higher-order correction δ_{ho} amounts to about 0.2% altogether and incidentally almost coincide with the QED correction. The finite- m correction $\delta_0 - 1$, of course, quenches $d\Gamma(H \rightarrow Z\tau^+\tau^-)/ds$ at threshold, but it is still as large as -1.7% at the upper endpoint, largely compensating the combined radiative

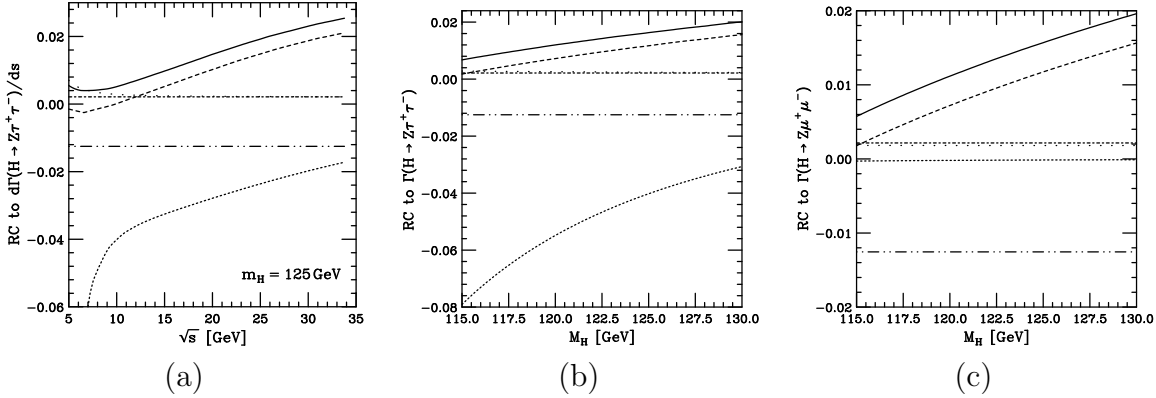


Figure 1: Tree-level finite- m (dotted lines) and radiative (solid lines) corrections to (a) $d\Gamma(H \rightarrow Z\tau^+\tau^-)/ds$ for $m_H = 125$ GeV as functions of the $\tau^+\tau^-$ invariant mass \sqrt{s} , and to (b) $\Gamma(H \rightarrow Z\tau^+\tau^-)$ and (c) $\Gamma(H \rightarrow Z\mu^+\mu^-)$ as functions of m_H . The radiative corrections include the $\mathcal{O}(\alpha)$ QED (coarsely dotted lines), $\mathcal{O}(\alpha)$ weak (dashed lines), and dominant higher-order (dot-dashed lines) corrections, of $\mathcal{O}(x_t^2)$, $\mathcal{O}(x_t\alpha_s)$, and $\mathcal{O}(x_t\alpha_s^2)$. For comparison, the $\mathcal{O}(\alpha)$ corrections predicted by the IBA (dot-dot-dashed lines) are also shown.

correction. As anticipated in Sec. 2.1, the relative contribution of y_0 to δ_0 , proportional to the $H\tau^+\tau^-$ coupling, is exceedingly small in magnitude, below 0.09%, over the full \sqrt{s} range. The finite- m corrections to $d\Gamma(H \rightarrow Z\mu^+\mu^-)/ds$ and $d\Gamma(H \rightarrow Ze^+e^-)/ds$ are negligible compared to the expected size of the presently unknown subleading higher-order corrections δ_{res} , and the radiative corrections to both observables are practically indistinguishable thanks to the almost perfect lepton universality. The latter are also very similar to the radiative corrections to $d\Gamma(H \rightarrow Z\tau^+\tau^-)/ds$, and we refrain from presenting the counterparts of Fig. 1(a) for $d\Gamma(H \rightarrow Z\mu^+\mu^-)/ds$ and $d\Gamma(H \rightarrow Ze^+e^-)/ds$.

Looking at Fig. 1(b), we observe that the finite- m correction to $\Gamma(H \rightarrow Z\tau^+\tau^-)$ ranges from -7.9% to -3.1% in the considered mass window $115 \text{ GeV} < m_H < 130 \text{ GeV}$ and more than compensates the overall radiative correction, which ranges there between 0.7% and 2.0%. From Fig. 1(c), we read off that the finite- m correction to $\Gamma(H \rightarrow Z\mu^+\mu^-)$ is below 0.03% in magnitude.

In Fig. 2(a), we present our best predictions for $d\Gamma(H \rightarrow Z\tau^+\tau^-)/ds$ (solid line) and $d\Gamma(H \rightarrow Z\mu^+\mu^-)/ds$ (dashed line) for $m_H = 125$ GeV as functions of \sqrt{s} including both finite- m and radiative corrections. For comparison, the tree-level result for $m = 0$ (dotted line) is also shown. The relation of the solid line shape to the dotted one may be easily understood from Fig. 1(a). The essential feature of the dashed line shape in comparison to the solid one is the insignificance of the finite- m correction for $\ell = \mu$ already mentioned above.

In Fig. 2(b), our best predictions for $\Gamma(H \rightarrow Z\tau^+\tau^-)$ (solid line) and $\Gamma(H \rightarrow Z\mu^+\mu^-)$ (dashed line) as functions of m_H are compared with the tree-level result for $m = 0$ (dotted line). The relative shifts of the solid and dashed line shapes with respect to the dotted

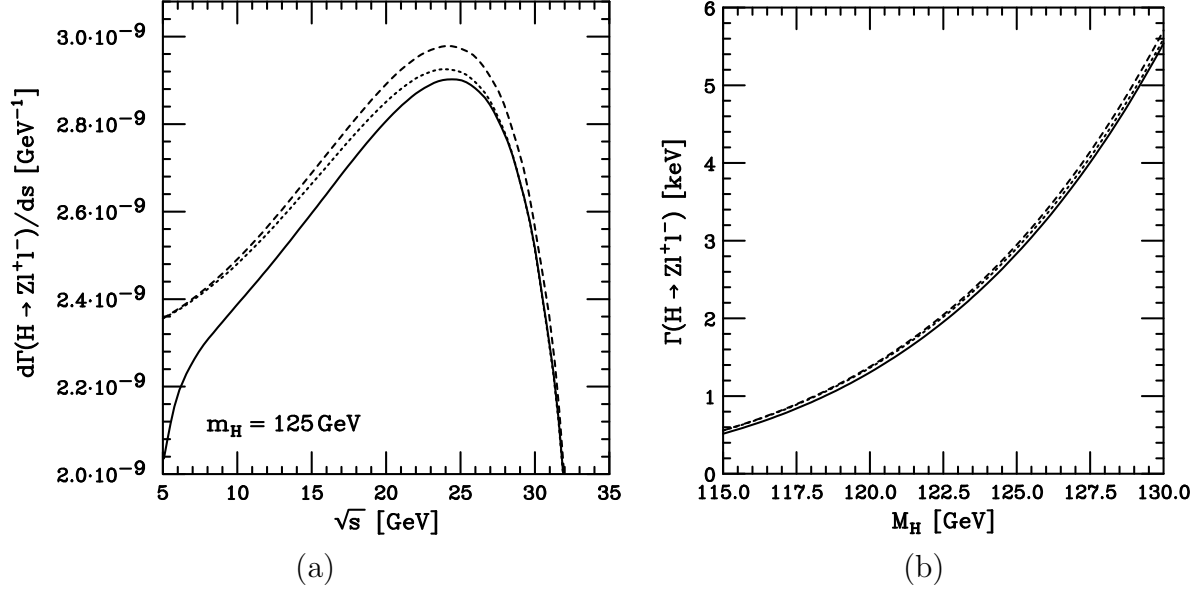


Figure 2: (a) $d\Gamma(H \rightarrow Z\ell^+\ell^-)/ds$ for $m_H = 125$ GeV as a function of the $\ell^+\ell^-$ invariant mass \sqrt{s} and (b) $\Gamma(H \rightarrow Z\ell^+\ell^-)$ as a function of m_H at the tree level for $m = 0$ (dotted lines) and including both finite- m and radiative corrections for $\ell = \mu$ (dashed lines) and $\ell = \tau$ (solid lines).

one immediately follow from Figs. 1(b) and (c), respectively.

We now turn to the $H \rightarrow W^+\ell^-\bar{\nu}_\ell$ decays. Figure 3 shows the tree-level finite- m (dotted lines) and radiative (solid lines) corrections to (a) $d\Gamma(H \rightarrow W^+\tau^-\bar{\nu}_\tau)/ds$ for $m_H = 125$ GeV as functions of \sqrt{s} , and to (b) $\Gamma(H \rightarrow W^+\tau^-\bar{\nu}_\tau)$ and (c) $\Gamma(H \rightarrow W^+\mu^-\bar{\nu}_\mu)$ as functions of m_H . The radiative corrections are built up by the $\mathcal{O}(\alpha)$ electroweak (dashed lines) and dominant higher-order (dot-dashed lines) corrections, of $\mathcal{O}(x_t^2)$, $\mathcal{O}(x_t\alpha_s)$, and $\mathcal{O}(x_t\alpha_s^2)$. For comparison, the $\mathcal{O}(\alpha)$ corrections predicted by the IBA (dot-dot-dashed lines) are also presented. Looking at Fig. 3(a), we observe that the electroweak correction δ_{ew} monotonically increases with \sqrt{s} , ranging from slightly negative values at the $\tau^-\bar{\nu}_\tau$ pair production threshold to about 4.5% at the upper endpoint. The one-loop electroweak correction is again inadequately described by the IBA term δ_{x_t} . The dominant higher-order correction δ_{ho} amounts to about 0.1% altogether.

Comparing Figs. 3(a)–(c) with Figs. 1(a)–(c), we observe that the finite- m corrections for the $H \rightarrow W^+\ell^-\bar{\nu}_\ell$ decays are significantly smaller than for the respective $H \rightarrow Z\ell^+\ell^-$ decays. This is mainly due to the fact that the shrinkage of the available phase space caused by switching on the finite- m corrections is lesser for the $H \rightarrow W^+\ell^-\bar{\nu}_\ell$ decays because the lepton pair production threshold is twice as low, at $\sqrt{s} = m$, and the upper endpoint is located higher, by $m_Z - m_W \approx 11$ GeV, also leading to correspondingly higher maxima of the \sqrt{s} distributions. In fact, the finite- m correction $\delta_0 - 1$ to $d\Gamma(H \rightarrow W^+\tau^-\bar{\nu}_\tau)/ds$ in Fig. 3(a) rapidly relaxes from its threshold value of -100% to moderate values, passing -1% at $\sqrt{s} \approx 8$ GeV and reaching -0.2% at the upper endpoint. As

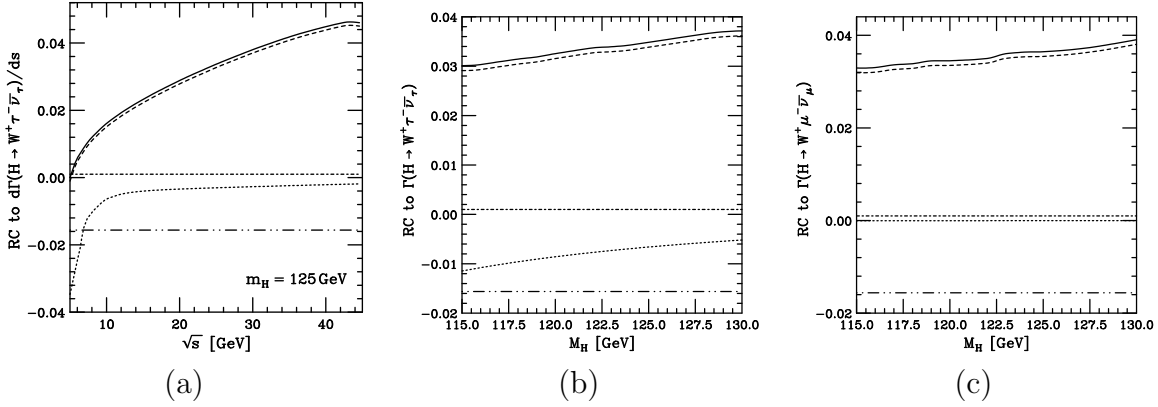


Figure 3: Tree-level finite- m (dotted lines) and radiative (solid lines) corrections to (a) $d\Gamma(H \rightarrow W^+\tau^-\bar{\nu}_\tau)/ds$ for $m_H = 125$ GeV as functions of the $\tau^-\bar{\nu}_\tau$ invariant mass \sqrt{s} , and to (b) $\Gamma(H \rightarrow W^+\tau^-\bar{\nu}_\tau)$ and (c) $\Gamma(H \rightarrow W^+\mu^-\bar{\nu}_\mu)$ as functions of m_H . The radiative corrections include the $\mathcal{O}(\alpha)$ electroweak (dashed lines) and dominant higher-order (dot-dashed lines) corrections, of $\mathcal{O}(x_t^2)$, $\mathcal{O}(x_t\alpha_s)$, and $\mathcal{O}(x_t\alpha_s^2)$. For comparison, the $\mathcal{O}(\alpha)$ corrections predicted by the IBA (dot-dot-dashed lines) are also shown.

anticipated in Sec. 2.2, the relative contribution of y_0 to δ_0 , proportional to the $H\tau^+\tau^-$ coupling, is very small, below 0.17%, over the full \sqrt{s} range.

From Fig. 3(b), we learn that the finite- m correction to $\Gamma(H \rightarrow W^+\tau^-\bar{\nu}_\tau)$ ranges from -1.1% to -0.5% in the considered mass window $115 \text{ GeV} < m_H < 130 \text{ GeV}$ and reduces the radiative corrections by between 38% to 14%. On the other hand, Fig. 3(c) tells us that the finite- m correction to $\Gamma(H \rightarrow W^+\mu^-\bar{\nu}_\mu)$ is absolutely negligible, being below 0.004% in magnitude.

In Fig. 4(a), our final predictions for $d\Gamma(H \rightarrow W^+\tau^-\bar{\nu}_\tau)/ds$ (solid line) and $d\Gamma(H \rightarrow W^+\mu^-\bar{\nu}_\mu)/ds$ (dashed line) for $m_H = 125$ GeV are shown as functions of \sqrt{s} and compared with the tree-level result for $m = 0$ (dotted line), so as to expose the interplay of the finite- m and radiative corrections. In Fig. 4(b), the same is done for $\Gamma(H \rightarrow W^+\tau^-\bar{\nu}_\tau)$ and $\Gamma(H \rightarrow W^+\mu^-\bar{\nu}_\mu)$ as functions of m_H .

4 Conclusions

We presented a precision study of the partial widths of the $H \rightarrow Z\ell^+\ell^-$ and $H \rightarrow W^+\ell^-\bar{\nu}_\ell$ decays including the full one-loop electroweak corrections and the dominant contributions at two and three loops, of $\mathcal{O}(x_t^2)$, $\mathcal{O}(x_t\alpha_s)$, and $\mathcal{O}(x_t\alpha_s^2)$. We also included finite- m corrections, which turned out to be indispensable for $\ell = \tau$, but negligible for $\ell = \mu, e$. Working in the on-mass-shell renormalization scheme with G_F replacing α as a basic parameter, we ensured that the radiative corrections remained moderate in size, being devoid of large logarithms involving small masses of charged fermions. As for the integrated partial decay widths, we found the net corrections relative to the tree-level

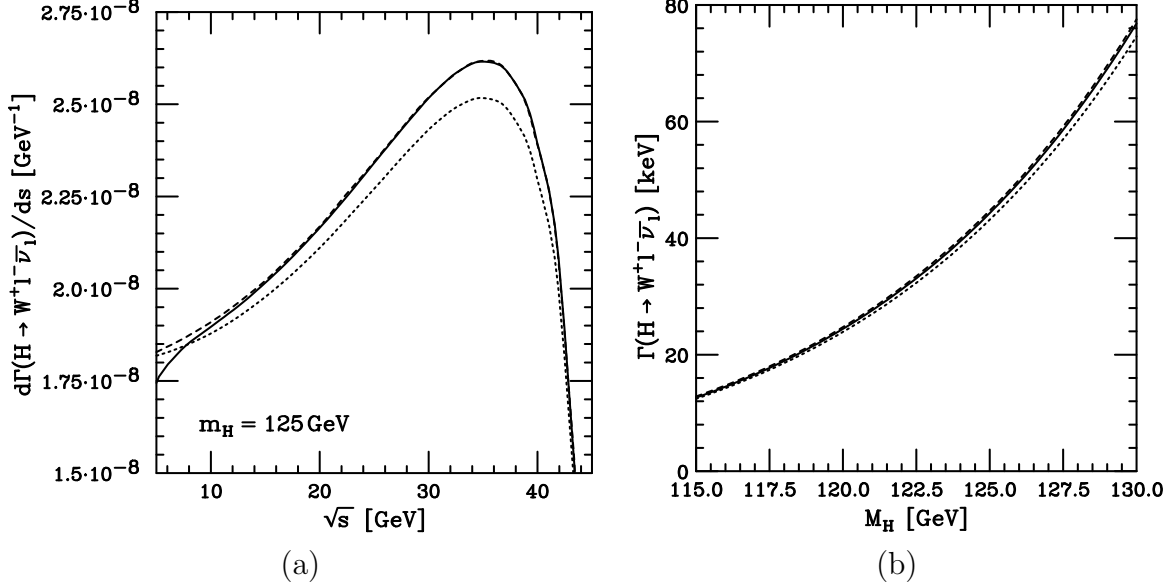


Figure 4: (a) $d\Gamma(H \rightarrow W^+\ell^-\bar{\nu}_\ell)/ds$ for $m_H = 125$ GeV as a function of the $\ell^-\bar{\nu}_\ell$ invariant mass \sqrt{s} and (b) $\Gamma(H \rightarrow W^+\ell^-\bar{\nu}_\ell)$ as a function of m_H at the tree level for $m = 0$ (dotted lines) and including both finite- m and radiative corrections for $\ell = \mu$ (dashed lines) and $\ell = \tau$ (solid lines).

results for $m = 0$ [49] at $m_H = 125$ GeV to be +1.6% for $H \rightarrow Ze^+e^-$ and $H \rightarrow Z\mu^+\mu^-$, -2.4% for $H \rightarrow Z\tau^+\tau^-$, +3.6% for $H \rightarrow W^+e^-\bar{\nu}_e$ and $H \rightarrow W^+\mu^-\bar{\nu}_\mu$, and +2.8% for $H \rightarrow W^+\tau^-\bar{\nu}_\tau$.

Acknowledgment

This work was supported in part by the German Federal Ministry for Education and Research BMBF through Grant No. 05H12GUE and by the Helmholtz Association HGF through Grant No. Ha 101.

References

- [1] G. Aad *et al.* (ATLAS Collaboration), Phys. Lett. B **710**, 49 (2012) [arXiv:1202.1408 [hep-ex]]; P. Mal (on behalf of the ATLAS Collaboration), arXiv:1206.1174 [hep-ex].
- [2] S. Chatrchyan *et al.* (CMS Collaboration), Phys. Lett. B **710**, 26 (2012) [arXiv:1202.1488 [hep-ex]]; M. Pieri (on behalf of the CMS Collaboration), arXiv:1205.2907 [hep-ex].
- [3] G. Davies *et al.* (The Tevatron New Phenomina and Higgs Working Group, CDF Collaboration, and D0 Collaboration), arXiv:1203.3774 [hep-ex].

- [4] R. Barate *et al.* (ALEPH Collaboration, DELPHI Collaboration, L3 Collaboration, OPAL Collaboration, and The LEP Working Group for Higgs Boson Searches) Phys. Lett. B **565**, 61 (2003) [hep-ex/0306033].
- [5] G. Aad *et al.* (ATLAS Collaboration), Phys. Lett. B **705**, 452 (2011) [arXiv:1108.5895 [hep-ex]]; Phys. Rev. Lett. **108**, 111803 (2012) [arXiv:1202.1414 [hep-ex]].
- [6] S. Chatrchyan *et al.* (CMS Collaboration), Phys. Lett. B **710**, 403 (2012) [arXiv:1202.1487 [hep-ex]].
- [7] G. Aad *et al.* (ATLAS Collaboration), Phys. Lett. B **705**, 435 (2011) [arXiv:1109.5945 [hep-ex]]; Phys. Lett. B **710**, 383 (2012) [arXiv:1202.1415 [hep-ex]].
- [8] S. Chatrchyan *et al.* (CMS Collaboration), arXiv:1202.1997 [hep-ex].
- [9] G. Aad *et al.* (ATLAS Collaboration), Phys. Rev. Lett. **108**, 111802 (2012) [arXiv:1112.2577 [hep-ex]]; arXiv:1206.0756 [hep-ex].
- [10] S. Chatrchyan *et al.* (CMS Collaboration), Phys. Lett. B **699**, 25 (2011) [arXiv:1102.5429 [hep-ex]]; Phys. Lett. B **710**, 91 (2012) [arXiv:1202.1489 [hep-ex]].
- [11] S. Chatrchyan *et al.* (CMS Collaboration), Phys. Lett. B **713**, 68 (2012) [arXiv:1202.4083 [hep-ex]].
- [12] S. Chatrchyan *et al.* (CMS Collaboration), Phys. Lett. B **710**, 284 (2012) [arXiv:1202.4195 [hep-ex]].
- [13] B. A. Kniehl, Phys. Rept. **240**, 211 (1994).
- [14] M. Spira, Fortsch. Phys. **46**, 203 (1998) [hep-ph/9705337]; B. A. Kniehl, Int. J. Mod. Phys. A **17**, 1457 (2002) [hep-ph/0112023]; A. Djouadi, Phys. Rept. **457**, 1 (2008) [hep-ph/0503172]; J. Ellis, M. K. Gaillard, and D. V. Nanopoulos, arXiv:1201.6045 [hep-ph].
- [15] J. R. Ellis, M. K. Gaillard, and D. V. Nanopoulos, Nucl. Phys. B **106**, 292 (1976); B. L. Ioffe and V. A. Khoze, Sov. J. Part. Nucl. **9**, 50 (1978) [Fiz. Elem. Chast. Atom. Yadra **9**, 118 (1978)]; M. A. Shifman, A. I. Vainshtein, M. B. Voloshin, and V. I. Zakharov, Sov. J. Nucl. Phys. **30**, 711 (1979) [Yad. Fiz. **30**, 1368 (1979)].
- [16] H.-Q. Zheng and D.-D. Wu, Phys. Rev. D **42**, 3760 (1990); A. Djouadi, M. Spira, J. J. van der Bij, and P. M. Zerwas, Phys. Lett. B **257**, 187 (1991); S. Dawson and R. P. Kauffman, Phys. Rev. D **47**, 1264 (1993); A. Djouadi, M. Spira, and P. M. Zerwas, Phys. Lett. B **311**, 255 (1993) [hep-ph/9305335]; K. Melnikov and O. I. Yakovlev, Phys. Lett. B **312**, 179 (1993) [hep-ph/9302281]; M. Inoue, R. Najima, T. Oka, and J. Saito, Mod. Phys. Lett. A **9**, 1189 (1994); J. Fleischer, O. V. Tarasov, and V. O. Tarasov, Phys. Lett. B **584**, 294 (2004) [hep-ph/0401090]; R. Harlander and P. Kant, JHEP **0512**, 015 (2005) [hep-ph/0509189].

- [17] M. Steinhauser, in *Proceedings of the Ringberg Workshop on the Higgs Puzzle—What can we learn from LEP2, LHC, NLC, and FMC?*, Ringberg Castle, Germany, 8–13 December 1996, edited by B.A. Kniehl (World Scientific, Singapore, 1997) p. 177 [hep-ph/9612395]; K. G. Chetyrkin, B. A. Kniehl, and M. Steinhauser, Nucl. Phys. B **510**, 61 (1998) [hep-ph/9708255].
- [18] U. Aglietti, R. Bonciani, G. Degrossi, and A. Vicini, Phys. Lett. B **595**, 432 (2004) [hep-ph/0404071].
- [19] A. Djouadi, P. Gambino, and B. A. Kniehl, Nucl. Phys. B **523**, 17 (1998) [hep-ph/9712330].
- [20] F. Fugel, B. A. Kniehl, and M. Steinhauser, Nucl. Phys. B **702**, 333 (2004) [hep-ph/0405232]; F. Fugel, Acta Phys. Polon. B **38**, 761 (2007) [hep-ph/0608303]; J. Brod, F. Fugel, and B. A. Kniehl, Phys. Rev. D **78**, 011303(R) (2008) [arXiv:0802.0171 [hep-ph]]; Nucl. Phys. B **807**, 188 (2009) [arXiv:0807.1008 [hep-ph]].
- [21] G. Degrossi and F. Maltoni, Nucl. Phys. B **724**, 183 (2005) [hep-ph/0504137]; G. Passarino, C. Sturm, and S. Uccirati, Phys. Lett. B **655**, 298 (2007) [arXiv:0707.1401 [hep-ph]].
- [22] E. Braaten and J. P. Leveille, Phys. Rev. D **22**, 715 (1980); N. Sakai, Phys. Rev. D **22**, 2220 (1980); T. Inami and T. Kubota, Nucl. Phys. B **179**, 171 (1981); M. Drees and K.-I. Hikasa, Phys. Lett. B **240**, 455 (1990); **262**, 497(E) (1991).
- [23] J. Fleischer and F. Jegerlehner, Phys. Rev. D **23**, 2001 (1981).
- [24] D. Yu. Bardin, B. M. Vilensky, and P. Kh. Khristova, Sov. J. Nucl. Phys. **53**, 152 (1991) [Yad. Fiz. **53**, 240 (1991)]; B. A. Kniehl, Nucl. Phys. B **376**, 3 (1992); A. Dabelstein and W. Hollik, Z. Phys. C **53**, 507 (1992).
- [25] S. G. Gorishnii, A. L. Kataev, S. A. Larin, and L. R. Surguladze, Mod. Phys. Lett. A **5**, 2703 (1990); Phys. Rev. D **43**, 1633 (1991); A. L. Kataev and V. T. Kim, Mod. Phys. Lett. A **9**, 1309 (1994).
- [26] L. R. Surguladze, Phys. Lett. B **341**, 60 (1994) [hep-ph/9405325].
- [27] B. A. Kniehl, Phys. Lett. B **343**, 299 (1995) [hep-ph/9410356].
- [28] K. G. Chetyrkin and A. Kwiatkowski, Nucl. Phys. B **461**, 3 (1996) [hep-ph/9505358].
- [29] B. A. Kniehl and A. Sirlin, Phys. Lett. B **318**, 367 (1993); B. A. Kniehl, Phys. Rev. D **50**, 3314 (1994) [hep-ph/9405299]; A. Djouadi and P. Gambino, Phys. Rev. D **51**, 218 (1995); **53**, 4111(E) (1996) [hep-ph/9406431].

- [30] A. Kwiatkowski and M. Steinhauser, Phys. Lett. B **338**, 66 (1994); **342**, 455(E) (1995) [hep-ph/9405308]; B. A. Kniehl and M. Spira, Nucl. Phys. B **432**, 39 (1994) [hep-ph/9410319]; B. A. Kniehl, Int. J. Mod. Phys. A **10**, 443 (1995) [hep-ph/9410330].
- [31] M. Butenschön, F. Fugel, and B. A. Kniehl, Phys. Rev. Lett. **98**, 071602 (2007) [hep-ph/0612184]; Nucl. Phys. B **772**, 25 (2007) [hep-ph/0702215].
- [32] K. G. Chetyrkin, Phys. Lett. B **390**, 309 (1997) [hep-ph/9608318].
- [33] K. G. Chetyrkin and M. Steinhauser, Phys. Lett. B **408**, 320 (1997) [hep-ph/9706462].
- [34] B. A. Kniehl and M. Steinhauser, Nucl. Phys. B **454**, 485 (1995) [hep-ph/9508241]; Phys. Lett. B **365**, 297 (1996) [hep-ph/9507382].
- [35] K. G. Chetyrkin, B. A. Kniehl, and M. Steinhauser, Phys. Rev. Lett. **78**, 594 (1997) [hep-ph/9610456]; Nucl. Phys. B **490**, 19 (1997) [hep-ph/9701277].
- [36] P. A. Baikov, K. G. Chetyrkin, and J. H. Kühn, Phys. Rev. Lett. **96**, 012003 (2006) [hep-ph/0511063].
- [37] A. L. Kataev and V. T. Kim, PoS (ACAT08), 004 (2008) [arXiv:0902.1442 [hep-ph]].
- [38] B. A. Kniehl, Phys. Lett. B **244**, 537 (1990); A. Grau, G. Panchieri, and R. J. N. Phillips, Phys. Lett. B **251**, 293 (1990).
- [39] B. A. Kniehl, Nucl. Phys. B **357**, 439 (1991).
- [40] B. A. Kniehl, Nucl. Phys. B **352**, 1 (1991).
- [41] D. Yu. Bardin, P. Kh. Khristova, and B. M. Vilensky, Sov. J. Nucl. Phys. **54**, 833 (1991) [Yad. Fiz. **54**, 1366 (1991)].
- [42] A. Bredenstein, A. Denner, S. Dittmaier, and M. M. Weber, Phys. Rev. D **74**, 013004 (2006) [hep-ph/0604011]; JHEP **0702**, 080 (2007) [hep-ph/0611234].
- [43] B. A. Kniehl, Phys. Rev. D **53**, 6477 (1996) [hep-ph/9602304].
- [44] B. A. Kniehl and M. Spira, Nucl. Phys. B **443**, 37 (1995) [hep-ph/9501392]; Z. Phys. C **69**, 77 (1995) [hep-ph/9505225].
- [45] B. A. Kniehl, Z. Phys. C **55**, 605 (1992); A. Denner, J. Küblbeck, R. Mertig, and M. Böhm, Z. Phys. C **56**, 261 (1992); A. Denner, B. A. Kniehl, and J. Küblbeck, DESY Report 92-123A (August 1992) p. 31.
- [46] S. Chatrchyan *et al.* (CMS Collaboration), JHEP **1203**, 081 (2012) [arXiv:1202.3617 [hep-ex]].
- [47] B. A. Kniehl, Phys. Lett. B **282**, 249 (1992).

- [48] T. G. Rizzo, Phys. Rev. D **22**, 722 (1980).
- [49] W. -Y. Keung and W. J. Marciano, Phys. Rev. D **30**, 248(R) (1984).
- [50] B. A. Kniehl, Comput. Phys. Commun. **58**, 293 (1990).
- [51] B. A. Kniehl, Nucl. Phys. B **347**, 86 (1990).
- [52] B. A. Kniehl and A. Sirlin, Nucl. Phys. B **371**, 141 (1992).
- [53] M. Consoli, W. Hollik, and F. Jegerlehner, in *Z Physics at LEP 1*, edited by G. Altarelli, R. Kleiss, and C. Verzegnassi, CERN Yellow Report No. 89-08 (September 1989) Vol. 1, p. 7; W. F. L. Hollik, Fortsch. Phys. **38**, 165 (1990); F. Halzen, B. A. Kniehl, and M. L. Stong, in *Particle Physics: VI Jorge André Swieca Summer School*, Campos de Jordão, Brasil, 14–26 January, 1991, edited by O.J.P. Éboli, M. Gomes, and A. Santoro (World Scientific, Singapore, 1992) p. 219; Z. Phys. C **58**, 119 (1993).
- [54] S. Dawson and S. Willenbrock, Phys. Lett. B **211**, 200 (1988).
- [55] M. Veltman, Nucl. Phys. B **123**, 89 (1977); M. B. Einhorn, D. R. T. Jones, and M. Veltman, Nucl. Phys. B **191**, 146 (1981).
- [56] J. J. van der Bij and F. Hoogeveen, Nucl. Phys. B **283**, 477 (1987); M. Consoli, W. Hollik, and F. Jegerlehner, Phys. Lett. B **227**, 167 (1989).
- [57] A. Djouadi and C. Verzegnassi, Phys. Lett. B **195**, 265 (1987); A. Djouadi, Nuovo Cim. A **100**, 357 (1988); B. A. Kniehl, J. H. Kühn, and R. G. Stuart, Phys. Lett. B **214**, 621 (1988).
- [58] L. Avdeev, J. Fleischer, S. Mikhailov, and O. Tarasov, Phys. Lett. B **336**, 560 (1994); **349**, 597(E) (1995) [hep-ph/9406363]; K. G. Chetyrkin, J. H. Kühn, and M. Steinhauser, Phys. Lett. B **351**, 331 (1995) [hep-ph/9502291].
- [59] K. Nakamura *et al.* (Particle Data Group Collaboration), J. Phys. G **37**, 075021 (2010).
- [60] K. G. Chetyrkin, B. A. Kniehl, and M. Steinhauser, Phys. Rev. Lett. **79**, 2184 (1997) [hep-ph/9706430]; Nucl. Phys. B **510**, 61 (1998) [hep-ph/9708255]; Y. Schröder and M. Steinhauser, JHEP **0601**, 051 (2006) [hep-ph/0512058]; K. G. Chetyrkin, J. H. Kühn, and C. Sturm, Nucl. Phys. B **744**, 121 (2006) [hep-ph/0512060]; B. A. Kniehl, A. V. Kotikov, A. I. Onishchenko, and O. L. Veretin, Phys. Rev. Lett. **97**, 042001 (2006) [hep-ph/0607202].